Multimodal Medical Image Fusion Using Dual-Tree Complex Wavelet Transform (DTCWT) with Modified Lion Optimization Technique (mLOT) and Intensity Co-Variance Verification (ICV)

C. G. Ravichandran [1] and Rubesh Selvakumar [2*]

[1] Department of Electronic and Communication Engineering
SCAD Institute of Technology, Trippur-641664, TamilNadu, India
cg_ravi@yahoo.com

[2] Department of Computer Science and Engineering
Madurai Institute of Engg. & Tech., Madurai, TamilNadu-630611, India
Seshind2014@gmail.com

Abstract ─ Image fusion is place as a key role in medical image investigation and preparation of treatments for bio-medical research and clinical diagnosis. The most incentive is fuse to capture a large amount of vital information from the input images to have its output image. In this paper, a well-organized multimodal medical image fusion approach is obtainable to fuse computer tomography (CT) and magnetic resonance image (MRI). The significant co-efficient of source images are line up through the dual-tree complex wavelet transform (DTCWT), followed by unit of low and high frequency components. Two completely different proposed fusion rules based on weighted fusion rule, the weights are optimized by modified lion optimization technique (mLOT) and intensity co-variance verification (ICV) are used to fuse the low and high frequency co-efficient. The fused image is reconstructed by inverse DTCWT with all amalgamate co-efficient. To prove the potency of the new approach is greater than the well-known standard algorithm, experiments are conducted. Based on experimental comparison and proposed approach, the better results are fused image quality are obtained. The studies of qualitative and quantitative metrics are clearly demonstrated that the new approach is to display the high superior than the present.

Index Terms ─ CT, DTCWT, ICV, low and high frequency, medical image fusion, mLOT, MRI.

I. INTRODUCTION

Multimodal medical image fusion refers to the identical and fusion between two or more images of the identical sight from single or different medical imaging modalities. The resultant image is acquired complementary information and makes it precise, further the ideal information is to help for the clinical diagnosis and treatment planning [1]. The aspiration of medical image fusion may be a single modality of medical image which cannot give the comprehensive and accurate information. And also, the physical process of integrating several modalities of medical images are rigorous, time overwhelming, human error and needs a lot of experiences. Therefore, different modality of medical images by automatic combining through the image fusion technique will acquire the complementary information employed in biomedical research and treatment planning of clinical diagnosis for doctors [2]. There are variety of medical images with individual application boundaries are together with the CT, MRI, PET and SPECT etc. Fusion of CT and MRI images will preserve far more edge and component information and produce a high quality fused image for doctors to obtain for accurate diagnosis. In worldwide, the multimodal medical image fusion grabs attention of specialists and scholars [3].

In dual approach for image fusion offered spatial domain and transform domain. The spatial domain oriented approach leads the pixel level to contrast reduction. Based on the subsequent approaches, Intensity-Hue-Saturation (IHS), Principal Component Analysis (PCA) and Brovey method supply higher results, however it suffers from the spectral degradation. In transform domain conjointly referred as multi-resolution, supported on pyramidal image fusion schemes fail to introduce any spatial orientation selectivity in the decomposition process and therefore usually cause blocking effects. Most of the above mentioned schemes with its own limitations [4-6].

In MRA technique of the discrete wavelet transform (DWT) will preserve spectral information powerfully; however, the spatial characteristics are not expressed in fine [7]. A huge vary of signal processing tasks will

Submitted On: December 10, 2015
Accepted On: February 29, 2016

apply effectively by the DWT. But its performance is inadequate of owing to the subsequent issues like, oscillations of the coefficients at a singularity, shift variance once tiny changes within the input cause giant changes within the output, aliasing is due to down sampling and non-ideal filtering throughout the analysis and a lack of directional selectivity in higher dimensions, i.e., distinguish between $+45^0$ and -45^0 edge orientations. An extensively best known methodology is to provide the shift invariance of the use of un-decimated quite, the dyadic filter tree that's required are most expeditiously with a tros algorithmic. On the conflicting furnish, the fully decimated DWT is smaller computational requirements than traditional and also conjointly exhibits high redundancy inside the yield information [8].

In the last decade, many software and systems are developed to employment the image fusion drawback. Those methods are based on multi-resolution transform fusion methods, have fascinated a significant quantity of research thought. An amount of accepted transforms embody the principal component analysis (PCA) [9], discrete wavelet (DWT) [10], stationary wavelet (SWT) [11], dual-tree complex wavelet [12], curvelet (CVT) [13], non sub-sampled contourlet transform (NSCT) [14], dual-tree complex wavelet with PSO (DTCWT-PSO) [15], non sub-sampled contourlet transform with SF_PCNN (NSCT_SF-PCNN) [5].

In this paper, a novel fusion skeleton is proposed for multimodal medical image fusions are supported on DTCWT fusion scheme. The core plan is to decompose the DTCWT on the source images followed by the fusion of low- and high-frequency coefficients. By incorporating the features of modified lion optimization technique (mLOT) and intensity co-variance verification (ICV) with the fusion rules for low- and high-frequency coefficients, in low frequency coefficients fusion that holds a number of significant information, can have an effect on the natural look of the fused results by using this fusion rule algorithm. It often used the weighted average fusion rule for the average low-frequency coefficients; it completely expected to diminish the contrast of the fused image in some extent. This paper is to conserve the region features and emphasize the different parts adaptively, exploitation the region based weighted average fusion rule is to fuse the low frequency coefficients. The weights are optimized with mLOA. In this technique, it is anticipated that the optimum fused results are adaptively intensity. The co-variance verification expeditiously verifies the frequency components from the high frequency coefficients. Grouping of these two will preserve the additional details of source images and improves the standard for fused images. The potency of the proposed framework is dispensed by the in-depth fusion experiments is totally different from multimodal CT/MRI and PET/SPECT/MRI dataset. Further, visual and quantitative analysis shows the proposed framework which provides a more robust fusion of outcome when the traditional image fusion technique applies.

The rest of this paper is organized as follows. Section II describes in the materials and methods, which includes summary of the DTCWT-PSO, primarily based image fusion theme is given and provides the procedure of the proposed technique. Section III provides the results and discussion followed by some experiments and conclusions in Section IV.

II. MATERIALS AND METHODS

This section covers the description of theory on which the future framework is based. These concepts include DTCWT which described as follows.

A. Dual-tree complex wavelet transform

Because of down-sampling a small change occurs within the input by DWT, it might cause aliasing immense within the wavelet coefficients. Inverse DWT revoke this aliasing offer, if the wavelet and scaling coefficients aren't changed [12]. And also, with shortcoming of DWT gives a deprived directional selectivity. These evils of real DWT are resolved using complex wavelets algorithm. However, complex wavelet decomposition of level 1 in perfect reconstruction creates a trouble. To conquer this, Kingsbury proposed the DT-CWT, which permit the perfect reconstruction, whereas it still provides the other benefits of complex wavelets [8].

The DT CWT makes use of two real DWT in its structure. The earliest DWT gives the real part of the transform and subsequent part gives the imaginary part. Filter banks of the analysis and synthesis are utilized in DT CWT are shown in Figs. 1 (a) and 1 (b) respectively. Two real wavelets transform use two completely different set of filters that satisfying the perfect reconstruction condition. It filters $h_o(n)$, $h_1(n)$, $g_0(n)$ and $g_1(n)$ denote the low pass/high pass filter pairs for the upper and lower filter banks respectively. Both filters are real but their mixture produces a complex wavelet. For fulfilling a perfect reconstruction condition the filters are intended to make a complex wavelet $\varphi(t) = \varphi_h(t) + j\varphi_g(t)$ approximately analytic by two real wavelet transforms $\varphi_h(t)$ and $\varphi_g(t)$. Consistently they are intended so that the lower wavelet $\varphi_g(t)$ is the Hilbert transform of upper wavelets $\varphi_g(t); \approx H\{\varphi_h(t)\}$.

In the inverse of DTCWT, the real part and imaginary part are all inverted and therefore, the inverse of the two real DWTs furnish a two real signal and to end with the average of two real signals gives a final output. We will acquire an inventive signal from either real part or imaginary part alone.

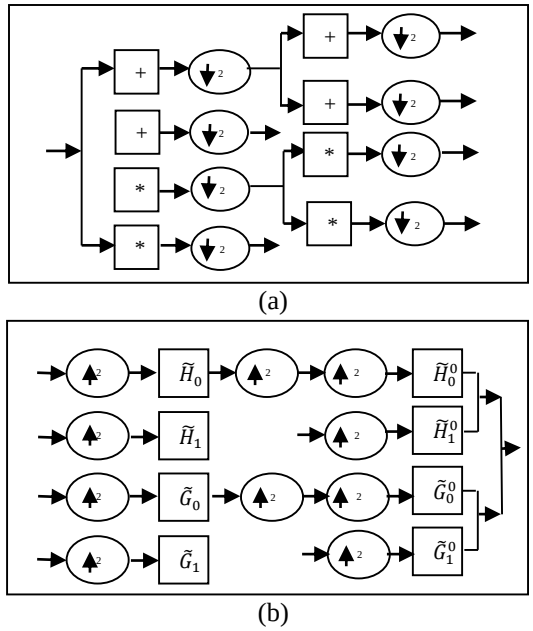

Fig. 1. (a) Analysis filter bank of DTCWT at two levels. (b) Synthesis filter bank of DTCWT at two levels.

B. Proposed fusion framework

In this section, the design and the approach of multimodal medical image fusion will be discussed. The proposed structure recognizes the modified lion optimization technique (mLOT) and intensity co-variance verification (ICV) in DTCWT domain, which acquires a couple of source image and to produce a combined image. The fundamental state in the proposed framework is that all the source images must be registered in order to align the matching pixels.

i. Modified lion optimization technique in DTCWT domain:

In general, finding the most optimal solution for problems in nature by humans under the guidance of several optimization techniques like genetic algorithm, ant colony optimization, honey bee optimization, bacterial foraging algorithm, teaching learning algorithm, particle swarm optimization, etc., to apply in different areas. However, none of the have proposed a technique to increase good number of optimal solution for all optimization problems. A few algorithms offer to improve the solutions for a little specific problem which compare with others. Therefore, the modified lion optimization pechnique [16] is based on a behavior of lion and social organization for applying in medical image fusion process for the purpose of the selection of optimal fusion weight of an image and the summarization of the process given below.

Step1: Initialization

To generate the populations (Lions) over the solution space in randomly,

$$Let\ f(L) = (x_1, x_2 \dots x_n) \text{ for } x_i,\ b_i,$$

where $a_i\ and\ b_i$ are lower and upper bound between 0 and 1, set and define in the all required parameters.

Step2: Hunting

a. Calculate the p based on the given formula of standard deviation and set in the p in center of the n(FH), where n(FH) is the number of female hunters:

$$\sigma = \sqrt{\frac{1}{N}\sum_{i=1}^{N}(x_i - \mu)^2}. \quad (1)$$

b. Set the female pride in some percentage for hunting and calculate the fitness value (β) [17,18], choose the best fitness to place on the center on the p and remaining are left and right of the center.

c. Select one after another female hunters randomly for attack the p. During this time D is added where, D is the disturbances of the hunters.

d. Once again estimate the fitness value of n(FH) and p then check and compare the previous and present and choose to best and discard the D.

e. Finally, move the p and n (FH) before that estimating the value of λ, where, λ is the variance of the p and H:

$$p' = p + R(0,1) \times \lambda \times (\mathrm{p} - \mathrm{FH}), \quad (2)$$

$$H' = \begin{cases} R(FH, p), if\ FH < p \\ R(p, FH), \quad FH > p \end{cases}. \quad (3)$$

Step3: Move to safe place

To move the safe place in the remaining female hunter and estimate the current and new position fitness value:

$$FH' = FH + C\big(R(0,1)\big) \times FH. \quad (4)$$

$$FH' = \begin{cases} \beta' \quad , if\ \beta < \beta' \\ \beta, otherwise \end{cases}. \quad (5)$$

where, C is the constant value between the 0 and 1.

Step4: Roaming

Select the male lion in the roaming and check if it is mad lion (ML) or nomad lion (NML). If it is ML, estimate the β current and new selected position in randomly:

$$ML' = \begin{cases} current\ \beta\ ,\ if\ current\ \beta > new\ \beta \\ new\ \beta, \qquad\qquad otherwise \end{cases}. \quad (6)$$

If the NML, estimate the probability of all using the given below equation:

$$Pr_i = 0.1 + \min\left(0.5, \frac{NML_i - best_{NML}}{best_{NML}}\right), i = 1,2 \dots, \quad (7)$$

$$NML_{ij} = \begin{cases} NML_j,\ if\ R_j > Pr_i \\ R_j, otherwise \end{cases}. \quad (8)$$

Step5: Mating

Set the female lion (FL) with all pride for mating to all male in the all pride and produce the two's c:

$$c_j, 1 = N \times FL_j + \sum \frac{(1-N)}{\sum_{i=1}^{NR} S_i} \times ML_j^i \times S_i, \quad (9)$$

$$c_j, 2 = 1 - N \times FL_j + \sum \frac{(N)}{\sum_{i=1}^{NR} S_i} \times ML_j^i \times S_i, \quad (10)$$

where, j is the dimension, $S_i = \begin{cases} 1, if\ male = i \\ 0, otherwise \end{cases}$ and N is the randomly generated numbers with a normal distribution with μ and σ, i.e., N(0,1).

Step6: Defense

To evaluate the β of mad and nomad of the male lion and choose the best using the given below Equation (11):

$$ML = \begin{cases} NML, if\ NML > ML \\ ML, otherwise \end{cases}. \quad (11)$$

Step7: Migration

Select in some of the mad female lion in equal for all pride to become a nomad and sort in the new and old nomad female using a sorting technique according to their β, then choose the best female among them randomly one after another to fill the empty place of the migrated female.

Step8: Equilibrium

Remove the worst β of the nomad with respect of the maximum permitted in the number of each gender in nomad.

Step9: Stopping criteria

Evaluate the best results and then stop the process based on the number of iterations.

ii. Intensity co-variance verification in DTCWT domain:

In general, fusion for high frequency coefficients which applies only the maximum selection rule for getting the absolute value, by applying this it doesn't consider the encircling pixels of image [Chandana *et al.*, 2011]. So, we propose a new unique fusion rule of intensity co-variance verification based on the local variance with the neighbors. The summarized process of this rule is as follows.

Step1:

After the decomposition process using DTCWT to get the high pass sub-bands $H_{l,d}^A(i,j)$ and $H_{l,d}^B(i,j)$ from images, they are split into 3x3 windows.

Step2:

Each window (both images) estimates the local mean value using the Equation (12):

$$\mu = \frac{1}{N} \sum_1^N (i,j). \quad (12)$$

Step3:

And then compute the local variance using the below Equation (13):

$$\sigma^2(X_{i,j}) = \frac{\sum_1^N (H_d^{A,B}(i,j) - \mu)^2}{N-1}, \quad (13)$$

where, N is no. of neighbor's data.

Step4:

Estimate the sum of variance is defined as:

$$sv = \sigma^2\left(H_d^A(i,j)\right) + \sigma^2\left(H_d^B(i,j)\right). \quad (14)$$

Step5:

Compute the percentage (p) of variances in both images using the Equation (15):

$$p = \sigma^2(H_d^{A,B}(i,j))/s. \quad (15)$$

Step6:

Finally, choose the best values between the 0 and 1 to the fused image.

iii. Fusion framework:

In this subsection the detailed enlightenment of the proposed fusion structure is considered by two absolute registered source images A and B. We proposed image fusion methods with two different modalities consisting of the subsequent steps:

Step1: Decomposition process

Perform the DTCWT decomposition process up to level n, to get two low frequency sub-bands and six high frequency sub-bands in each level. These sub-bands are defined as:

$$\{(L_t^A(i,j), H_{l,d}^A(i,j)\ :\ l = n, t = 1,2, d = 1 \ldots 6\},$$

$$\{(L_t^B(i,j), H_{l,d}^B(i,j)\ :\ l = n, t = 1,2, d = 1 \ldots 6\},$$

where $L_t^A(i,j), L_t^B(i,j)$ the low frequency sub-bands in the t orientation are, $H_{l,d}^A(i,j) H_{l,d}^B(i,j)$ represent the high frequency sub-bands *l* level in the *d* orientation and show the DWT coefficients of CT and MRI in Figs. 2 (a) and 2 (b).

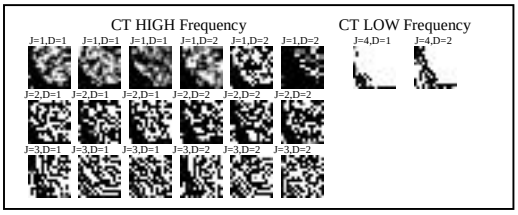

(a)

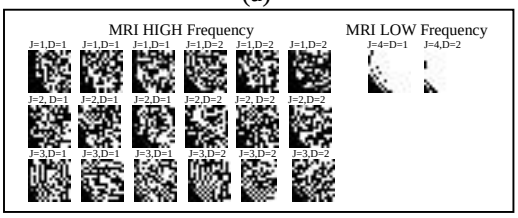

(b)

Fig. 2. (a) DTCWT coefficients for low and high in the first image at 3 levels. (b) DTCWT coefficients for low and high in the second image at 3 levels.

Step2: Segmentation process

A number of segmentation algorithms are obtainable in the literature [19] for thresholding and clustering. This algorithm usually generates undesired segmented regions, throughout the existing paper, the low pass sub-bands are segmented by the normalized cut [20, 21] image segmentation and it shows the segmented process in Fig. 3.

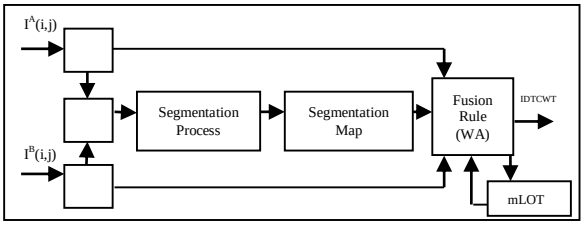

Fig. 3. Segmentation process in low frequency coefficients.

Based on segmentation approach, the low frequency coefficients of both source images are segmented by the region and to get a better segmentation.

Step3: Fusion of low frequency sub images

The low-frequency sub images of the coefficients will be a character of the approximation component of the source images. The traditional averaging methods are used to construct the composite bands. However, it cannot provide the fused low-frequency component of high quality for medical image. As a result, it leads to the economical contrast within the fused images. So, one simplest way is to use the pixel based weighted average fusion rule to present the fused coefficients, the weights are taken as a value between 0 and 1. In general, the weights value will be 0.5. However, this process is suitable only for the same modality and it won't fuse multi-modal images as various dynamic ranges; PBAVE can considerably alter the intensity range of the images and it reduces the contrast within the fused image. Therefore, a contemporary principle is proposed on region-based fusion rules employed by manipulating the measures of the significance of a region as a priority and choosing with the higher priority in the analogous region. The source images features of the regions are preserved, but the optimal results couldn't be obtained by merely selecting coefficients from one input. So, the weights are optimized by mLOA and the process will be described as Section III.A;

$$L_{F,R_k}(i,j) = w_k \times L^A_{t,R_k}(i,j) + (1 - w_k) \times L^B_{t,R_k}(i,j), \quad (16)$$

where $L_{F,R_k}(i,j)$ denotes the fused coefficients of R_k corresponding to $L^A_{t,R_k}(i,j)$ and $L^B_{t,R_k}(i,j)$.

Step4: Fusion of high frequency sub images

Generally, the high-frequency sub-image coefficients takes up fine detail components with the source image. Because the fusion process will have an effect on the fusion performance as a result of its notable, that the noise is additionally involved in high frequency and will cause fault of sharpness.

Therefore, a brand new criterion is proposed here, based on intensity co-variance verification. In general, the most choice of maximum selection rule accustomed construct the composite bands; however, this rule doesn't take any thought of the surrounding pixels. Therefore, a completely unique approach is proposed by intensity verification. This rule is employed to elaborate I^A (i, j) I^B(i, j).

Step5:

Perform inverse DTCWT on the composite low- and high-frequency sub-bands up to n levels to obtain the fused image F and the information flow, the diagram of proposed image fusion algorithm is shown in Fig. 4.

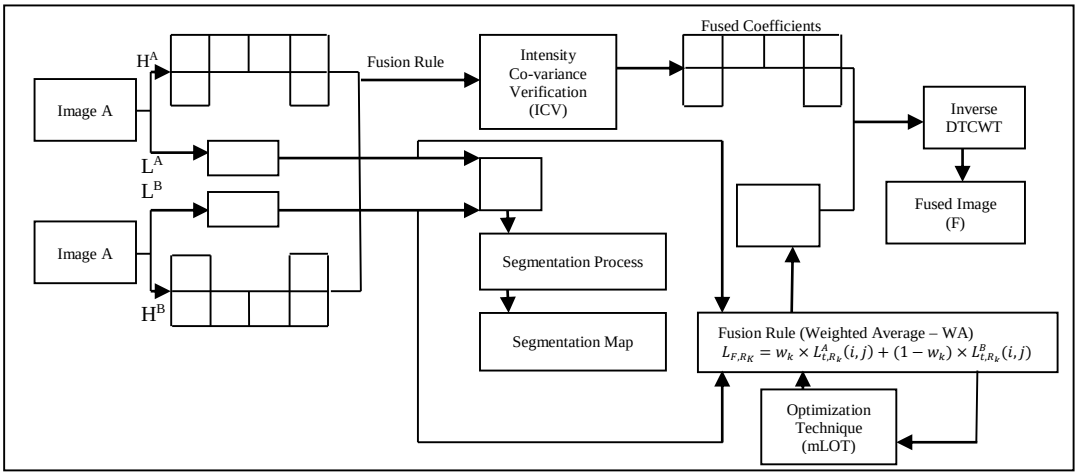

Fig. 4. Block diagram of information flow of proposed multimodal medical image fusion framework.

III. RESULTS AND DISCUSSIONS

It has been developed with MATLAB 15a for simulation of image fusion algorithms, many versions obtainable, however a new version of Math work 15a is an additional feature for the present work such as sub-version supply management integration, advanced new graphic systems etc. In general, MATLAB is an interactive program for numerical computations and information image, used extensively by management engineers for analysis and it support to completely different operational systems like UNIX, Windows etc. Here, are a few reasons to choosing the MATLAB 15a during this analysis work as provides several functions, enable one to make sure top numerical preciseness, commanding mathematical and geometric support for the implementing of superior algorithms over ever, helpful to loosen the matter with matrix and vectors formulation of the present work.

In general, the CT image will offer bone dense structures and implants with a smaller amount of falsity, but it cannot discover physiological changes. The MRI image will present customary and pathological soft tissue data; however, it cannot read the position of bones information and CT-MRI images to be fused can yield a combined image with the contents and MRI fusion of proton density and weighted images of T2 place in harmonizing image details to the results of fusion. During this case, one image may not be capable to offer precise clinical requirements for the physicians. Therefore, needed for the multimodal medical image fusion and it has secured. The simulation results can exhibit fusion of these multimodal images, get a composite fused image consisting of complementary information from varied image modalities. The earlier depends on human visual characteristics and additionally the expert knowledge of the viewer, hence fuzzy, time-consuming and poor-repeatable. However these are typically correct if performed properly. The alternative one is comparatively formal and simply accomplished by the computer algorithms that typically valuate the similarity between the fused and source images. However, choosing a proper consistent criterion with the subjective assessment of the image quality is rigorous. Hence, there is a desire to form an evaluation system. Therefore, primary an evaluation index system is recognized to gauge the proposed fusion algorithm. These indices are determined consistent with the statistical parameters.

A. Performance of proposed system using the quality metrics

i. Standard Deviation (SD):

This metric is additionally efficient in the lack of noise. It deals with the contrast in the fused image. An image with high contrast would have a high standard deviation [22]. The statistical moment $_{MF}$ is the fused image histogram *(f)* is defined as:

$$M_F = \sum_{i=0}^{n-1}(f_i - m)^2 p(f_i), \quad (17)$$

where m is the average intensity, n is the maximum possible intensity levels and $P(f_i)$ is the probability of specific level i occurs in fused image. Average m intensity is defined as:

$$M = \sum_{i=0}^{n-1} f_i p(f_i^{''}). \quad (18)$$

Standard deviation σ can be defined as the second moment about mean [12]:

$$\sigma = \sqrt{M_2(f)}. \quad (19)$$

The metric based on standard deviation (σ) can be successfully implemented in noise free situation. Average contrast in fused image is represented by standard deviation. There is direct variation between the standard deviation and the amount of contrast in the given image.

ii. Structural Similarity Index Metric (SSIM):

Structural similarity is intended by modeling some image deformation as the combination of loss of correlation, radiometric and contrast distortion. Mathematically, SSIM between two variables U and V is defined as [23]:

$$SSIM(U,V) = \frac{\sigma_{UV}}{\sigma_U \sigma_V} \frac{2\mu_U \mu_V}{\mu_U^2 \mu_V^2} \frac{2\sigma_U \sigma_V}{\sigma_U^2 \sigma_V^2}, \quad (20)$$

where μ_U, μ_V mean intensity, σ_U, σ_V and σ_{UV} are the variances and covariance respectively. Based on the definition of SSIM, a new way to use SSIM for the image fusion assessment is proposed in [23] and is defined as:

$$Q_S = \begin{cases} \lambda(w) SSIM(A, F/w + \big(1 - \lambda(w)\big) SSIM(B, F/w), \\ \qquad if\ SSIM(A, B/w) > 0.75 \\ \max\left[SSIM\left(A, \frac{F}{w}\right),\ SSIM\left(B, \frac{F}{w}\right)\right] \\ \qquad if\ SSIM\left(B, \frac{F}{w}\right) < 0.75\ , \end{cases} \quad (21)$$

where w is a sliding window of size, which moves pixel by pixel from the top-left to the bottom-right corner and λ (w) is the local weight obtained from the local image salience.

iii. Normalized Mutual Information (NMI):

It is a quantitative appraise of the mutual dependence of two variables [24]. It typically illustrates measurement of the information shared by two images. Mathematically, MI between two discrete random variables U and V is defined as:

$$MI(U,V) = \sum_{u \in U} \sum_{v \in V} p(u,v) \log_2 \frac{p(u,v)}{p(u)P(v)}, \quad (22)$$

where $p(u,v)$, the joint probability distribution function of U and V, whereas $p(u)$ and $p(v)$ are the marginal probability distribution functions of U and V respectively. Based on the above definition, the quality

of the fused image with respect to input images A and B can be expressed as:

$$Q_{MI} = 2\left[\frac{MI(A,F)}{H(A)+H(F)} + \frac{MI(B,F)}{H(B)+H(F)}\right], \quad (23)$$

where H(A), H(B) and H(F) is the marginal entropy of images A,B and F respectively.

iv. Edge Similarity Index Measure (ESIM):

It provides the similarity between the edges transferred in the fusion process. Mathematically, $Q^{AB/F}$ is defined as [23]:

$$Q^{AB/F} = \left(\sum_{i=1}^{M}\sum_{j=1}^{N}\left[Q_{i,j}^{AF} w_{i,j}^{x} + Q_{i,j}^{BF} w_{i,j}^{x}\right]\right) / \left(\sum_{i=1}^{M}\sum_{j=1}^{N}\left[w_{i,j}^{x} + w_{i,j}^{x}\right]\right), \quad (24)$$

where A, B and F represents the input and fused images respectively. The definition of Q^{AF} and Q^{BF} are same and given as:

$$Q_{i,j}^{AF} = Q_{g,i,j}^{AF} Q_{\alpha,i,j}^{AF} \qquad Q_{i,j}^{BF} = Q_{g,i,j}^{BF} Q_{\alpha,i,j}^{BF}, \quad (25)$$

where Q_{gj}^{F} and Q_{α}^{F} are the edge strength and orientation preservation values at location (i,j) respectively for images. The dynamic range for $Q^{AB/F}$ is [0, 1] and it should be close to 1 as possible for better fusion.

B. Experiments on CT/MRI image fusion

Evaluation and the performance of the image fusion are proposed in these rules with six sets. And is perfectly registered in CT-MRI images and the MR-T1-MR-T2 images are experimented with few collection of fusion algorithms. All the images shown in Fig. 5 is in the size of 256 × 256 pixel and then applied to the given datasets by numerous existing and proposed algorithms are delivered from the complete brain image database, which furnish the free access of images for educational and research purpose [25]. After this validation, we demonstrated the potential of our fusion rule to fuse other modalities. In addition, it is consulted with the radiologist, this proposed approach gives enhanced information and also it will be useful for medical applications like medical diagnosis etc. for doctors.

With high opinion to several imaging state and principles, the source images with different modalities have complementary information. Based on these, all the image groups are proposed fusion results are good to compared with the some acceptable existing and present approaches. The assessment of statistical parameters for the fused images is totally varied from the fusion algorithms and it is shown in the Table 1, visually in Fig. 6 and graphically in Figs. 7 (a), 7 (b), 7 (c) and 7 (d) separately because of clear variation of the parameters representation. Based on the graph, figure and the table, the proposed algorithm is obvious, preserves spectral information and also improves the spatial detail information to the overall existing algorithm, which can be easily observed to obtain the maximum values of evaluation indices of SD, NMI, SSIM and ESIM. The values of the all techniques based on the above performance indices with respect to fusion for existing and the proposed, the proposed value of all are higher and occurs it gives a better quality fused image compared with the others.

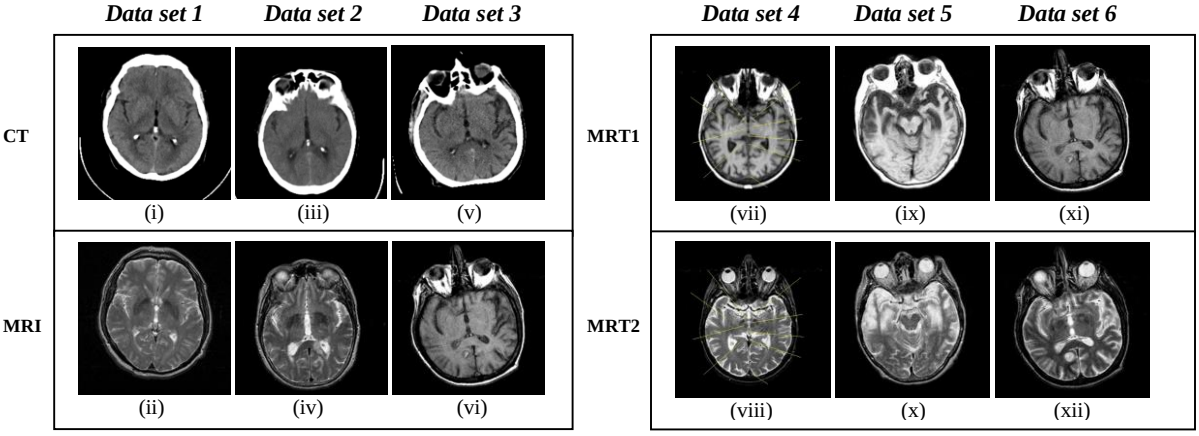

Fig. 5. Multimodal medical image data sets: (i), (iii) and (v) CT image; (ii), (iv) and (vi) MRI image; (vii), (ix) and (xi) MR-T1 image; (viii), (x) and (xii) MR-T2 image.

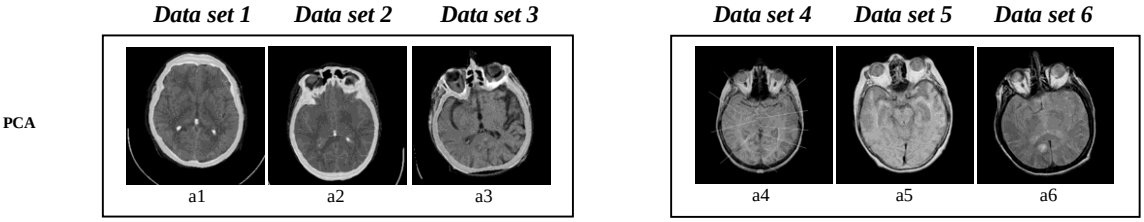

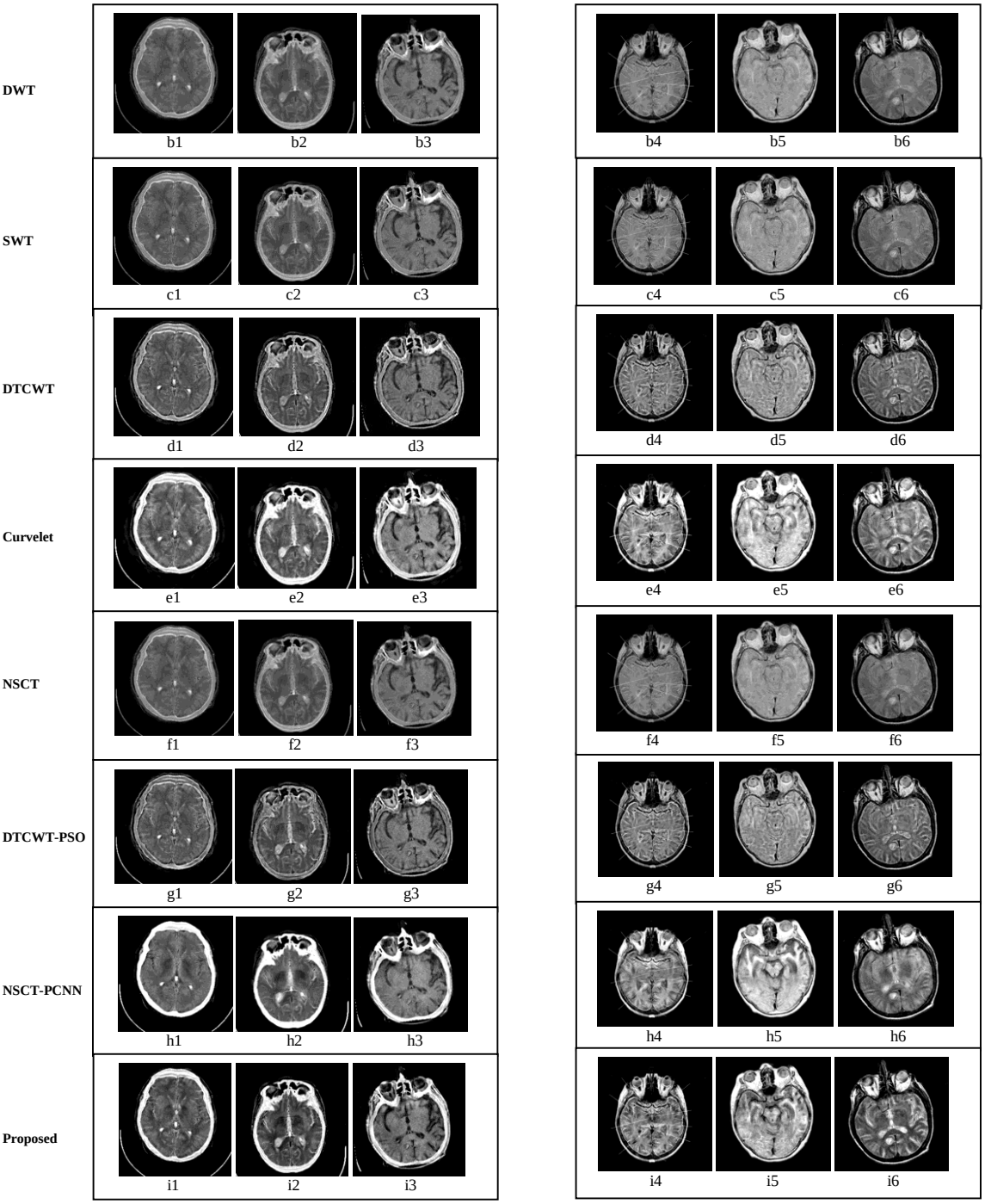

Fig. 6. The multimodal medical image fusion results of different fusion algorithms: fused images from (a1-a6) PCA based technique; (b1-b6) DWT based technique; (c1-c6) SWT based technique; (d1-d6) DTCWT based technique; (e1-e6) curvelet based technique; (f1-f6) NSCT based technique; (g1-g6) DTCWT-PSO based technique; (h1-h6) NSCT-PCNN based technique; (i1-i6) proposed technique.

Table 1: Evaluation performance for fused medical images by various quality metrics

Image Modality	Quality Metrics	PCA	DWT	SWT	DTCWT	Curvelet	NSCT	DTCWT PSO	NSCT PCNN	Proposed
Data Set I CT and MRI	SD	62.884	55.0227	55.847	58.5727	75.736	70.658	56.9724	77.2038	72.8881
	NMI	0.826	0.7169	0.715	0.6729	0.5861	0.5967	0.6851	0.7702	0.8411
	SSIM	4.607	4.6522	3.819	3.1969	3.0688	3.948	3.1142	3.2844	4.0761
	ESIM	0.401	0.3406	0.455	0.5068	0.4746	0.4897	0.5003	0.448	0.5717
Data Set II CT and MRI	SD	63.467	56.7274	57.426	60.6093	79.482	72.7865	56.8767	79.817	74.805
	NMI	0.838	0.7665	0.782	0.7301	0.6181	0.6452	0.7563	0.7327	0.8849
	SSIM	3.935	4.0307	3.46	3.0475	3.1377	3.324	2.9442	3.2801	4.0905
	ESIM	0.378	0.3493	0.454	0.5223	0.5179	0.5185	0.5068	0.4829	0.5677
Data Set III CT and MRI	SD	63.153	60.4157	61.312	64.5094	81.59	70.6423	63.2617	80.0196	75.8832
	NMI	0.826	0.7426	0.747	0.697	0.5934	0.5825	0.712	0.7882	0.801
	SSIM	3.965	3.8432	3.28	2.9357	3.0886	3.2749	2.8732	3.1825	4.0091
	ESIM	0.369	0.359	0.436	0.4884	0.4531	0.4659	0.4817	0.4376	0.5692
Data Set IV MRT1 and MRT2	SD	59.079	58.3354	58.88	62.4244	76.8882	71.231	62.313	72.6492	77.2225
	NMI	0.791	0.7696	0.792	0.767	0.6736	0.6834	0.7743	0.7242	0.8238
	SSIM	3.462	3.3427	3.124	2.8843	3.0368	3.2398	2.8944	3.0745	2.9086
	ESIM	0.337	0.3331	0.417	0.5154	0.4787	0.4946	0.5176	0.4414	0.5419
Data Set V MRT1 and MRT2	SD	76.316	74.2201	74.686	76.6255	95.4531	73.462	74.9361	93.2302	97.2543
	NMI	0.825	0.7503	0.739	0.6919	0.7147	0.7351	0.7017	0.8612	0.8931
	SSIM	4.126	3.8884	3.558	3.3027	3.4823	3.5127	3.2398	3.6406	4.4269
	ESIM	0.449	0.4394	0.473	0.5068	0.4688	0.4759	0.5007	0.5027	0.5618
Data Set VI MRT1 and MRT2	SD	57.28	57.1453	57.836	60.7211	72.9397	67.359	60.9295	68.6153	74.8084
	NMI	0.752	0.7779	0.775	0.7737	0.6875	0.6938	0.7745	0.7323	0.8502
	SSIM	3.829	3.9184	3.582	3.2526	3.3334	3.239	3.2672	3.3183	4.3012
	ESIM	0.437	0.4385	0.467	0.5282	0.5015	0.5128	0.5297	0.4705	0.5677

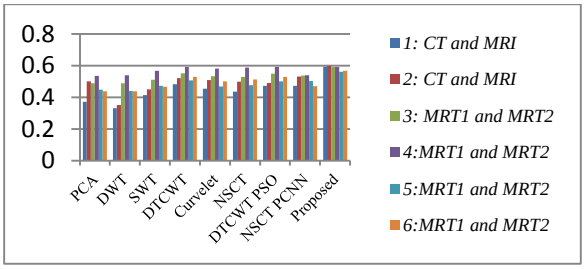

(a)

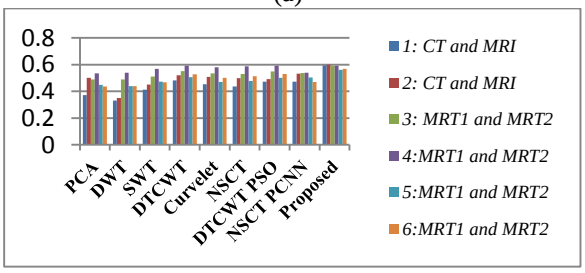

(b)

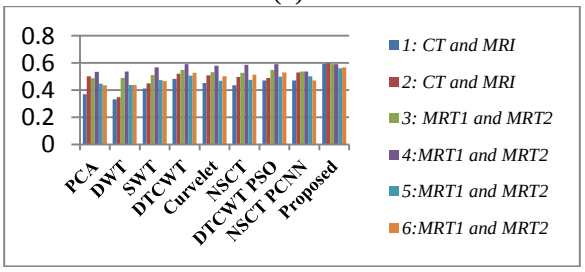

(c)

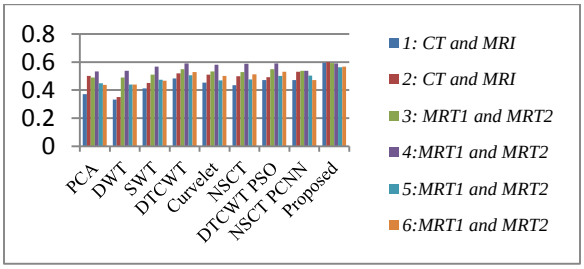

(d)

Fig. 7. (a) Variation of performance parameters with various fusion methods based on standard deviation. (b) Variation of performance parameters with various fusion methods based on NMI. (c) Variation of performance parameters with various fusion methods based on SSIM. (d) Variation of performance parameters with various fusion methods based on ESIM.

By the experimental images, PCA based schemes offer underprivileged results comparative to other techniques. Because it has no scale selectivity and it is not obvious to deal properly with incomplete data set, in which some of the points are missing. To overcome this inadequacy it satisfied the pyramid and multi resolution based algorithms. However, the fused image contrast will be reduced comparatively less in multi resolution based algorithms. With multi

resolution based algorithms, the NSCT based algorithm performs better result because the NSCT is a multi-scale geometric analysis tool which utilizes the geometric regularity in the image and provides an asymptotic optimal representation in the terms of better localization, multi-direction and shift invariance. This is also justified by the fact that shift-invariant decomposition overcomes successfully and improves the quality of the fused image around the edges. This approach is to perform some extent well supported multi-focus images. However, in this algorithm the medical images give not as much of performance. For the reason that, it is not able to present in the low-frequency efficiently by prominent information and to obtain the poor results [15].

The performance of this proposed method [26] is close to each other, it is to furnish the fine quality fused images compared to other fused results that suffers to others the obtained fused result which suffers something noticeably to reduce the visual quality, time consuming and also missing some information due to initial level decomposition process. In this proposed approach it is based on spatial frequency and pulse coupled neural network [16]. By looking carefully in the fused image the internal edges are missing (weak edges) and also computational time is very long. So, the key motivation of the proposed approach gives a better performance to extract a more accurate and prominent information from low and high frequency coefficients, the time reducing and the supplementary accepted output with improved visual quality. Thus, it can be concluded from Fig. 6 and Table 1 proves the superiority of the proposed method over existing methods based on visual and statistical assessment.

C. Real clinical examples on CT/MRI, and MR-T1/MR-T2 image fusion

The performance of clinical diagnosis, the CT and MRI image fusion at the semi-oval center area is essential. CT images hold anatomical information, and MRI images offer the normal and pathological soft tissue. The proposed fusion rules in multimodal medical image fusion becomes a growing study and analysis for doctors to find a more precise diagnosis. Figure 8 shows the real clinical images of the two sets of CT and MRI and the MRT1 and MRT2 are considered to demonstrate the practical value of the proposed scheme. The first case of a 25 year young human who is investigated through the CT scan for neuroestithelical tumor but not in the clear visible for those scanned in Fig. 8 (i). However, in the MRI image of the same patient will find some notable symptoms but recovery is critical because of visual difficultly. In the second case is of a 47 year old woman who one day was not able to speak and was weak on the right side of the body. Then she was admitted in the hospital and the doctors investigated through the CT image but it indicated as normal. However, the doctors had a doubt for this patient and also the image. After 3 days the doctors were initiate acquired in the MRI. They observed large area of abnormal signal in the region in MRI image. Here in early analysis is compared with the existing techniques, the proposed technique can be observed in the all information in the fused image and also gives a better quality within the high contrast image shown in the Table 2, visually displayed in Fig. 9, and the illustration by the graph in the Figs. 10 (a), 10 (b), 10 (c) and 10 (d) independently on the basis of standard deviation, NMI, SSIM and ESIM.

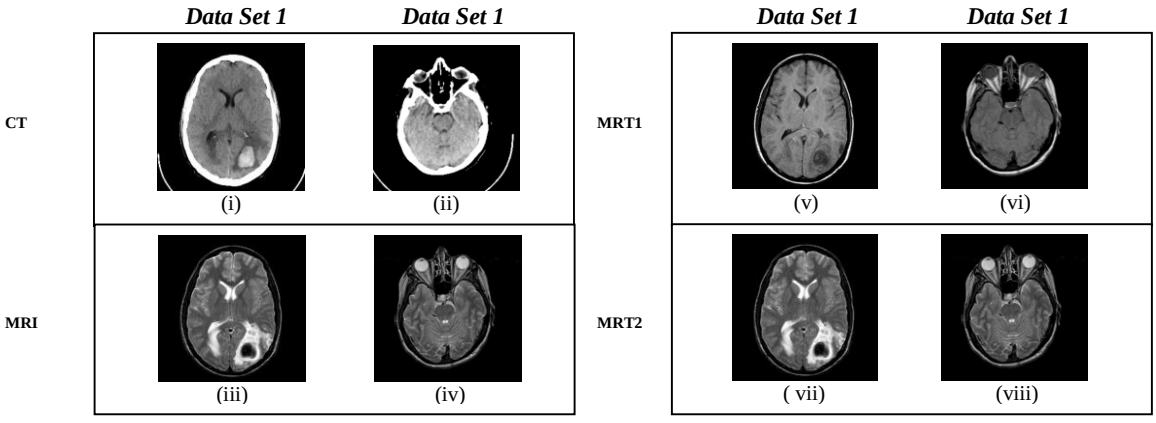

Fig. 8. Real clinical multimodal medical image data sets: (i) and (iii) CT image; (ii) and (iv) MRI image; (v) and (vii) MR-T1 image; (vi) and (viii) MR-T2 image.

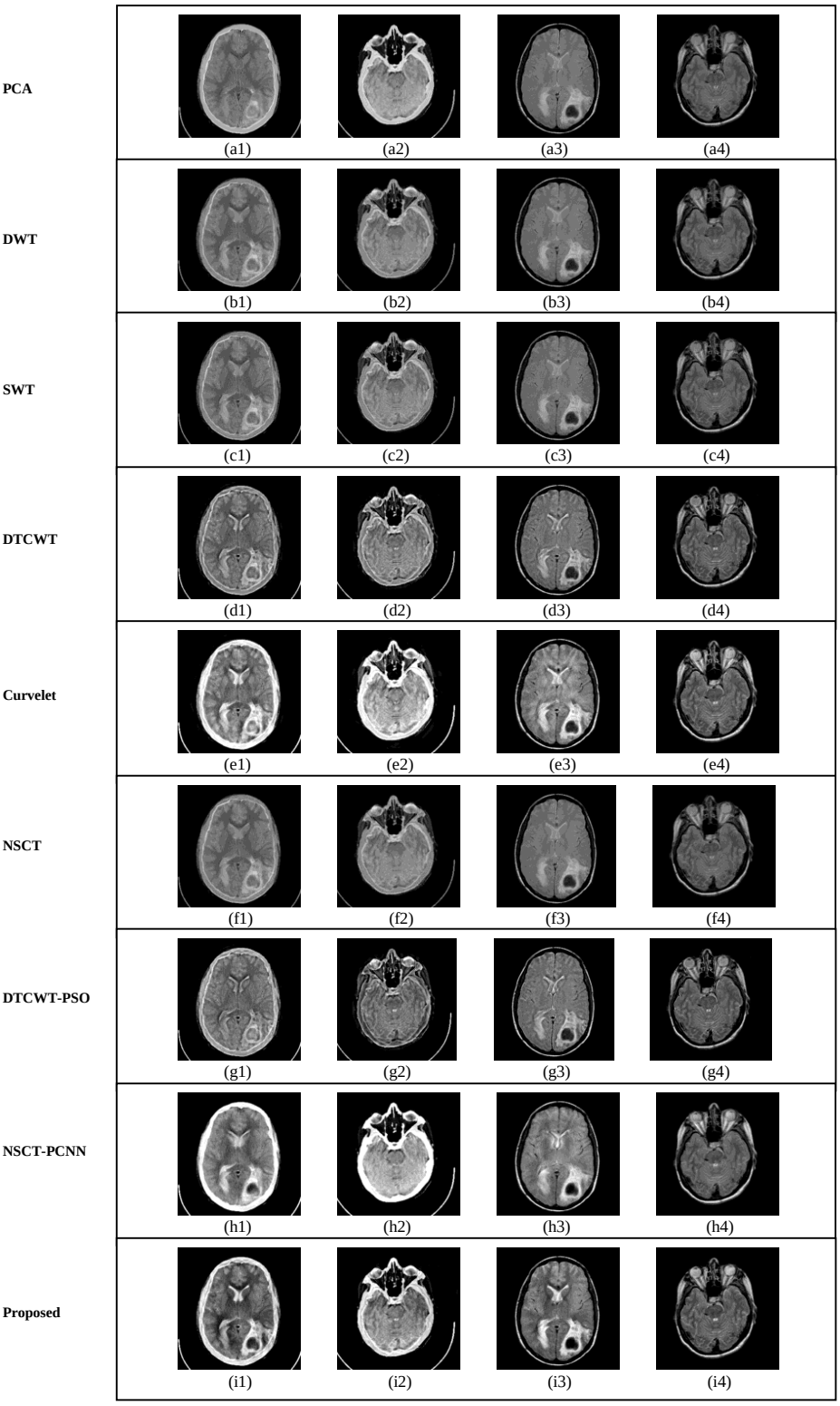

Fig. 9. The multimodal medical image fusion results of different fusion algorithms: fused images from (a1-a4) PCA based technique; (b1-b4) DWT based technique; (c1-c4) SWT based technique; (d1-d4) DTCWT based technique; (e1-e4) curvelet based technique; (f1-f4) NSCT based technique; (g1-g4) DTCWT-PSO based technique; (h1-h4) NSCT-PCNN based technique; (i1-i4) proposed technique.

Table 2: Evaluation performance for fused medical images by various quality metrics

Image Modality	Quality Metrics	PCA	DWT	SWT	DTCWT	Curvelet	NSCT	DTCWT PSO	NSCT PCNN	Proposed
Data Set I CT and MRI	SD	65.541	61.4685	61.959	63.7885	75.4965	70.7653	66.9167	76.1149	75.3883
	NMI	0.848	0.7625	0.76	0.7005	0.6456	0.6574	0.6898	0.8063	0.8872
	SSIM	3.922	3.782	3.397	3.0492	3.3196	3.9724	3.1482	3.5409	4.3167
	ESIM	0.371	0.3315	0.413	0.4827	0.4535	0.4354	0.4723	0.4717	0.5943
Data Set II CT and MRI	SD	77.253	63.4617	64.19	67.3	80.6006	72.3864	58.6839	81.6084	84.0422
	NMI	4.001	3.6725	3.031	2.6375	2.8586	3.0585	2.5432	3.1672	3.7301
	SSIM	3.9530	3.5482	3.6548	3.0682	3.4231	3.9832	3.3652	3.6384	4.5372
	ESIM	0.501	0.3502	0.451	0.5203	0.5093	0.4982	0.491	0.5312	0.5981
Data Set III MRT1 and MRT2	SD	58.012	58.1103	58.617	60.6151	60.9098	56.4582	60.7721	61.7255	64.5669
	NMI	0.816	0.821	0.809	0.7792	0.7276	0.6894	0.7783	0.8169	0.8863
	SSIM	3.599	3.6302	3.382	3.124	3.2239	3.5632	3.118	3.1891	4.1816
	ESIM	0.489	0.4893	0.511	0.5501	0.5338	0.5287	0.549	0.5379	0.5915
Data Set IV MRT1 and MRT2	SD	46.64	46.684	47.023	48.4167	49.4354	43.5734	48.4333	50.5065	51.4235
	NMI	0.894	0.9	0.912	0.891	0.8616	0.7943	0.8906	0.879	0.9854
	SSIM	3.671	3.7543	3.515	3.1996	3.2501	3.8734	3.1966	3.3043	4.1543
	ESIM	0.534	0.5381	0.567	0.5911	0.5805	0.5873	0.5908	0.5382	0.5909

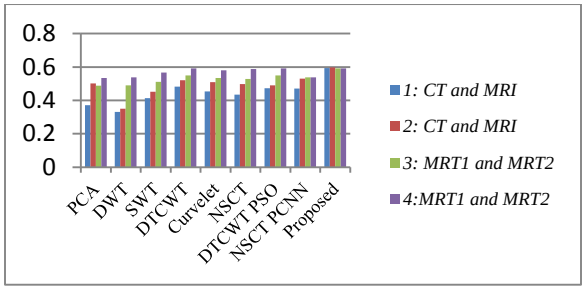

(a)

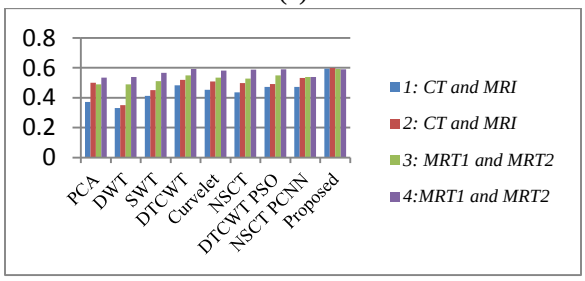

(b)

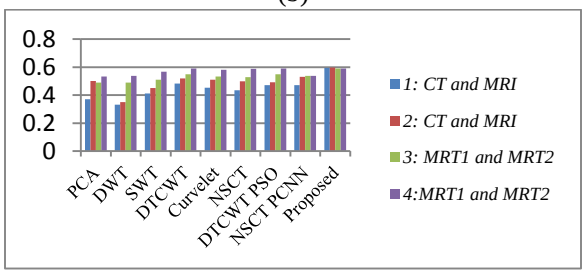

(c)

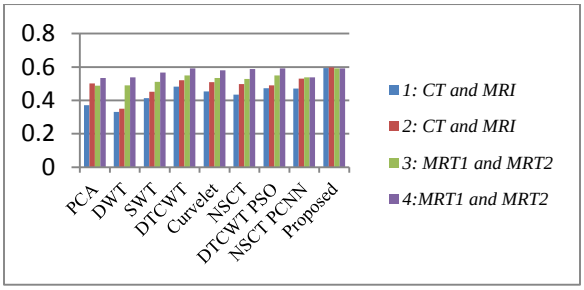

(d)

Fig. 10. (a) Variation of performance parameters with various fusion methods based on standard deviation. (b) Variation of performance parameters with various fusion methods based NMI. (c) Variation of performance parameters with various fusion methods based SSIM. (d) Variation of performance parameters with various fusion methods based ESIM.

IV. CONCLUSION

In this paper, new unique image fusion rules are proposed for multi-modal medical images, which is based on dual tree complex wavelet transform with modified LOA and ICV for the low pass sub-bands and high pass sub-bands. In our experimental results, several groups of CT and MRI and MRT1and MRT2 images are fused based on a few standard acceptable existing algorithms and the new unique proposed systems. The visual and statistical comparisons

demonstrate that the performance of the proposed algorithm is superior to the existing state-of-the-art methods. Proposed approach can improve the details of the fused image, and can get better effect of the visual quality with a smaller amount information distortion than existing methodologies. In the real applications, it will precisely offer an additional detail for diagnosis by doctors based on our new approach with the properties of high quality, high flexibility and time consumption. However, all modality of imaging has its own sensible limitations. In the follow-up study, a numerous work can be implemented in the new medical image fusion approach. From the variety of image quality estimation table and graphs, it has been obvious that the proposed fusion technique outperforms in terms of standard deviation, normalized mutual Information, structure similarity index measure and edge similarity index measure.

REFERENCES

[1] J. H. Teng, X. Wang, J. Zhang, S. Wang, and P. Huo, "A multimodality medical image fusion algorithm based on wavelet transform," *International Conference on Advances in Swarm Intelligence*, 6146:627-633, 2010.

[2] S. Das and M. K. Dundu, "A neuro-fuzzy approach for medical image fusion," *IEEE Transaction on Bio-medical Engineering*, vol. 60, no. 12, pp. 3347-3353, 2013.

[3] Z. Lu, H.-P. Yiu, Y. Chai, S. X. Yang, "A novel approach for multi-modal medical image fusion," *Experts Systems with Applications*, vol. 41, no. 16, pp. 7425-7435, 2014.

[4] V.S. Retronic and S. Xydias, "Gradient based multi-resolution image fusion," *IEEE TIP*, vol. 13, no. 2, pp. 228-237, 2004.

[5] Z. Wang and Y. Ma, "Medical image fusion using m-PCNN," *Information Fusion*, vol. 9, no. 2, pp. 176-185, 2008.

[6] S. Das and M. K. Kund, "NSCT based multi-modal medical image fusion using pulse coupled neural network and modified spatial frequency," *Medical and Biological Engineering and Computing*, vol. 50, no. 10, pp. 1145-1114, 2012.

[7] T. Yong, S. S. Park, S. Huang, and N. Rao, "Medical image fusion via an effective wavelet based approach," *EURASIP Journal of Advance in Signal Processing*, pp. 1-13, 2010.

[8] Kingsbury, "The dual-tree complex wavelet transform: A new technique for shift invariance and directional filters," *IEEE Digital Signal Processing Workshop*, 1998.

[9] V. P. S. Naidu and J. R. Raol, "Pixel-level image fusion using wavelets and principal component analysis," *Defense Science Journal*, vol. 58, no. 3, pp. 338-352, 2008.

[10] Q. Guihong, Z. Dali, and Y. Pingfan, "Medical image fusion by wavelet transform modulus maxima," *Opt. Express*, vol. 9, pp. 184-190, 2001.

[11] T. J. Li and Y. Y. Wang, "Biological image fusion uses a SWT based variable-weights selection scheme," *In Proc. of the 3rd International Conference on Bioinformatics and Biomedical Engineering*, pp. 1-4, 2009.

[12] I. W. Selesnick, R. G. Baraniuk, and N. G. Kingsbury, "The dual tree complex wavelet transform: A coherent framework for multi-scale signal and image processing," *IEEE Signal Processing Magazine*, vol. 22, no. 6, pp. 123-151, 2005.

[13] F. E. Ali, I. M. El-Dokany, A. A. Saad, and F. E. Abd El-Samie, "Curvelet fusion of mr and ct images," *Progr. Electromagn. Res. C*, vol. 3, pp. 215-224, 2008.

[14] M Q. Zhang and B. L. Guo, "Multi-focus image fusion using the non-sub-sampled contourlet transform," *Signal Process*, vol. 89, no. 7, pp. 1334-1346, 2009.

[15] J. Tao, S. Li, and B. Yang, "Multimodal image fusion algorithm using dual-tree complex wavelet transform and particle swarm optimization," *Advanced Intelligent Computing Theories and Application Communications in Computer and Information Science*, vol. 93, pp. 296-303, 2010.

[16] M. Yazdani and F. Jolai, "Lion optimization algorithm (LOA): A nature-inspired meta heuristic algorithm," *Journal of Computational Design and Engineering*, vol. 1, pp. 1-12, 2015.

[17] C. C. Lai, C. H. Wu, and M. C. Tsai, "Feature selection using particle swarm optimization with application in spam filtering," *International Journal of Innovative Computing Information and Control*, vol. 5, pp. 423-432, 2009.

[18] G. Piella and H. Heijmans, "A new quality metric for image fusion," *In Proc. of International Conference on Image Processing*, 2:173-6-III, 2003.

[19] R. Xu and D. Wunsch, "Survey of clustering algorithms," *IEEE Transactions on Neural Networks*, vol. 6, no. 3, pp. 645-678, 2005.

[20] J. Shi and J. Malik, "Normalized cuts and image segmentation," *IEEE Transactions on Pattern Analysis and Machine Intelligence*, vol. 22, no. 8, pp. 888-905, 2000.

[21] S. Li and B. Yang, "Multi-focus image fusion using region segmentation and spatial frequency," *Image and Vision Computing, Elsevier*, vol. 26, pp. 971-979, 2008.

[22] G. N. Raut, P. L. Paikrao, and D. S. Chaudhari, "Study of quality assessment techniques for fused images," *International Journal of Innovative*

Technology and Exploring Engineering, vol. 2, pp. 290-294, 2013.
[23] C. Yang, J. Zhang, X. Wang, and X. Liu, "A novel similarity based quality metric for image fusion," *Inf. Fusion*, vol. 9, pp. 156-160, 2008.
[24] G. Bhatnagar, Q. M. J. Wu, and Z. Liu, "Directive contrast based multimodal medical image fusion in NSCT domain," *IEEE Transaction on Multimedia*, vol. 15, no. 5, pp. 1014-1024, 2013.
[25] http://www.med.harvard.edu/AANLIB/
[26] Y. Chai, H. Li, and X. Zhang, "Multi-focus image fusion based on features contrast of multi-scale products in non sub-sampled contourlet transform domain," *Optik*, vol. 123, pp. 569-581, 2012.

C. G. Ravichandran received his B.E. degree in Electronics and Communication Engineering from Bharathiyar University in 1988 and M.E. degree in Electronics Engineering and Ph.D. degree in Information and Communication Engineering (Medical Image Processing) from Anna University, Chennai during 1991 & 2009 respectively. Currently he is the Professor & Principal of SCAD Institute of Technology, Palladam, Tamilnadu, India. He has produced Four Ph.D.'s so far and currently guiding Eight Ph.D. candidates in Anna University Chennai. He has published around 20 articles in various reputed international Journals. His research interests include image segmentation, medical image processing, network architecture, distributed systems and web services.

Rubesh Selvakumar received the MCA degree from MK Universities, Madurai, TamilNadu, India in 2001 and M.E. degree from Anna University, Chennai, TamilNadu, India in 2005. He was a part time Research Fellowship with the Image Processing, Anna University, and Chennai. He has published many papers and presented in the conference in various areas like image processing, MANET and Wireless Communications. He is currently an Asst. Professor with the Department of Computer Science and Engineering, MIET, Madurai, TamilNadu, India. His research interests lie on the broad area of image processing with application in medical image fusion and noising analysis.